

## Retraction

# Retracted: The Research on Intelligent Measurement Terminal of Water-Saving Irrigation Based on RN2026 Microcontroller

### Journal of Sensors

Received 23 January 2024; Accepted 23 January 2024; Published 24 January 2024

Copyright © 2024 Journal of Sensors. This is an open access article distributed under the Creative Commons Attribution License, which permits unrestricted use, distribution, and reproduction in any medium, provided the original work is properly cited.

This article has been retracted by Hindawi following an investigation undertaken by the publisher [1]. This investigation has uncovered evidence of one or more of the following indicators of systematic manipulation of the publication process:

- (1) Discrepancies in scope
- (2) Discrepancies in the description of the research reported
- (3) Discrepancies between the availability of data and the research described
- (4) Inappropriate citations
- (5) Incoherent, meaningless and/or irrelevant content included in the article
- (6) Manipulated or compromised peer review

The presence of these indicators undermines our confidence in the integrity of the article's content and we cannot, therefore, vouch for its reliability. Please note that this notice is intended solely to alert readers that the content of this article is unreliable. We have not investigated whether authors were aware of or involved in the systematic manipulation of the publication process.

Wiley and Hindawi regrets that the usual quality checks did not identify these issues before publication and have since put additional measures in place to safeguard research integrity.

We wish to credit our own Research Integrity and Research Publishing teams and anonymous and named external researchers and research integrity experts for contributing to this investigation.

The corresponding author, as the representative of all authors, has been given the opportunity to register their agreement or disagreement to this retraction. We have kept a record of any response received.

### References

- [1] R. Guo, S. Liu, X. Liu, B. Liu, and Z. Gu, "The Research on Intelligent Measurement Terminal of Water-Saving Irrigation Based on RN2026 Microcontroller," *Journal of Sensors*, vol. 2023, Article ID 6832321, 12 pages, 2023.

## Research Article

# The Research on Intelligent Measurement Terminal of Water-Saving Irrigation Based on RN2026 Microcontroller

Runzhou Guo,<sup>1</sup> Shujie Liu,<sup>1</sup> Xiaoxiao Liu,<sup>1</sup> Beilei Liu,<sup>1</sup> and Zhanlei Gu <sup>2</sup>

<sup>1</sup>State Grid Xingtai Power Supply Company, Xingtai, Hebei 054000, China

<sup>2</sup>Henan XJ Metering Co., Ltd., Xuchang, Henan 461000, China

Correspondence should be addressed to Zhanlei Gu; [guzhanlei128@163.com](mailto:guzhanlei128@163.com)

Received 24 August 2022; Revised 10 October 2022; Accepted 15 October 2022; Published 20 April 2023

Academic Editor: Yuan Li

Copyright © 2023 Runzhou Guo et al. This is an open access article distributed under the Creative Commons Attribution License, which permits unrestricted use, distribution, and reproduction in any medium, provided the original work is properly cited.

Water-saving irrigation technology has been studied for many years, but due to insufficient investment in research and development of irrigation equipment, it cannot be effectively promoted and applied. In order to improve the water use efficiency of farmland irrigation, the automatic monitoring of groundwater level change, soil moisture change, and crop seasonal growth status is realized in the ditch or pump well irrigation area. An intelligent measuring terminal for water-saving irrigation based on RN2026 microcontroller is developed. The terminal uses the coefficient of “water conversion by electricity” to automatically convert the water consumption of farmers and uses the price mechanism of water rights to affect farmers’ water conservation. In combination with changes in groundwater level, crop evapotranspiration, and dynamic changes in soil moisture, precision irrigation strategies are automatically generated to guide farmers to use water rationally. Through the function and performance experiments, the results show that the error of the coefficient of “water conversion by electricity” is less than 1%, the error of electric energy measurement is less than 0.5%, the estimated value of average water use right per unit arable area is consistent with the actual value, and the predicted value of daily average soil moisture change is consistent with the measured value. The equipment has strong adaptability to the environment, high measurement accuracy, strong data processing ability, low cost, and other characteristics. It meets the requirements of water-saving irrigation technology in practical applications and has good promotion and application value.

## 1. Introduction

In northern China, natural rainfall usually cannot meet the needs of crop growth, and pumping groundwater or ditch water for irrigation is the decisive factor for stable and high yield of crops [1]. In recent years, the proportion of agricultural irrigation water has become higher and higher, causing the groundwater level to drop year by year, which has a great impact on the local climate and environment [2]. Therefore, it is necessary to further strengthen the intelligent construction of agricultural water-saving irrigation measurement terminal, improve the efficiency of agricultural irrigation water, and realize the sustainable development of agricultural irrigation.

At present, most irrigation intelligent measurement devices charge by swiping the card, by installing a card reader module inside the smart electricity meter, or connect-

ing the card reader module outside the data collector. Wang et al. developed the remote water and electricity metering equipment for agricultural motor wells and used radio frequency identification technology to complete the accurate management of water use in irrigation areas [3]. Li et al. designed an intelligent double control system of water and electricity for agricultural irrigation well house. Through a four-layer distributed partial closed loop structure, the charge management for water and electricity in one card is realized [4]. Liu et al. designed an intelligent control system for wireless irrigation of seedlings based on ARM and STM32 and realized high-precision agricultural irrigation based on S3C2410A microprocessor and mobile data services [5]. The results show that these methods mainly solve the household metering problem of farmers’ irrigation electricity. However, due to the high investment cost of agricultural irrigation metering equipment, the lack of water right

restraint mechanism, crop growth status monitoring, soil moisture monitoring, and other measures, the farmers have not formed a precise irrigation strategy to guide farmers. Farmers often rely on experience to flood irrigation, resulting in serious waste of water resources.

In view of the high investment cost of agricultural irrigation metering facilities and the inability to monitor crop growth status, soil moisture status, groundwater level status, and water right constraint mechanism in real time, this paper adopts the method of “water conversion by electricity” based on water flow velocity to measure water consumption in real time through irrigation electricity consumption, replacing the traditional water meter metering method [6]. With the intelligent measurement terminal equipment as the carrier, it can sense the agricultural growth state, soil moisture, groundwater level, power consumption data, irrigation water volume, and other data; formulate accurate irrigation strategies according to the water level changes, water right indicators, and soil moisture in different regions; and guide farmers to conduct scientific irrigation and save water, which is of great significance for the sustainable development of agricultural irrigation [7].

## 2. The Overall Design of Intelligent Measurement Terminal System

The intelligent measurement terminal system is mainly composed of RN2026 microcontroller, AC sampling circuit, LCD module, card swiping button module [8], motor control, data storage module, water level monitoring, and soil moisture monitoring module; the overall system architecture is shown in Figure 1.

During the operation of intelligent measurement terminal, the microcontroller collects the change of groundwater level through the water level monitoring module, drives the servo motor according to the water level change limit set by the user, and makes the groundwater pump handle the reasonable position [9]. After the farmer swipes the card and presses the key, the alternating current sampling circuit inputs the voltage and current signals to the RN2026 microcontroller, which calculates the power consumption of each farmer’s irrigation, and calculates the farmer’s water consumption through the “water conversion by electricity” coefficient. The electricity consumption process and fee deduction of farmers are displayed by liquid crystal display [10]. The soil moisture monitoring module is used to monitor the change of soil moisture content in real time and timely remind farmers of scientific irrigation according to the preset precision irrigation strategy. The power consumption data and water consumption data of farmers are reported to the power consumption information acquisition system through 4G module or broadband carrier module.

## 3. The Hardware Design of Intelligent Measurement Terminal

*3.1. The Design and Analysis of Main Control Circuit.* Due to the poor operating environment of the intelligent measurement terminal, it operates in high temperature, high humid-

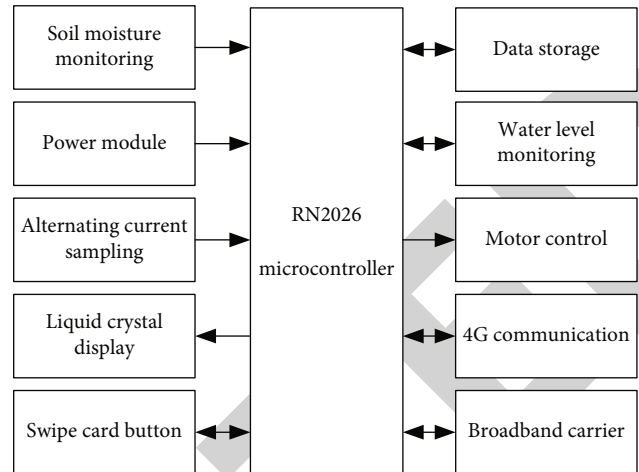


FIGURE 1: Architecture diagram of intelligent measurement terminal system.

ity, and other environments for a long time. Document 3 uses STM32F103 chip, which has the advantages of the highest clock frequency, large storage capacity, and rich peripheral interface resources and the disadvantages of no metering function, requiring external electricity meters and water meters [3]. Document 5 uses S3C2410A chip, which has the advantages of high performance, flexible configuration, and strong data processing capability. The disadvantage is that it requires external power and water sensors, and the system stability is poor [5]. In view of the above reasons, the main control circuit of this terminal selects a RN2026 microcontroller with high integration, wide voltage of 2.8 V~5.5 V, high accuracy, high reliability, and low power consumption, and the power error is less than 0.1%. The chip integrates arm Cortex-M0 core, 256 Kb flash, 48 KB SRAM, 7-channel  $\Sigma$ - $\Delta$ ADC, three-phase metering and fault detection module, metering accuracy self-detection module, four-way multiplexed SAR ADC, eight-way multiplexed GP-ADC, independent power supply hardware temperature compensation RTC, a variety of communication peripheral interfaces, etc., which are applicable to the metering, communication, control, and other functions and performance requirements of the well irrigation measurement terminal [11].

The traditional water metering method needs to install a water meter, which is costly and requires a lot of maintenance. In order to save costs and improve the reliability of the product, this paper selects the RN2026 chip with the electric energy metering function to realize the water metering function through the “water conversion by electricity” algorithm and avoid installing water meters and other metering equipment.

The intelligent measurement terminal adopts the modular design method, collects the voltage and current signals of motor well irrigation in real time through the AC sampling module, and uses the RN2026 built-in measurement algorithm to accumulate the electric energy data in real time. The peripheral circuit of the microcontroller RN2026 is configured with card swiping module, liquid crystal display

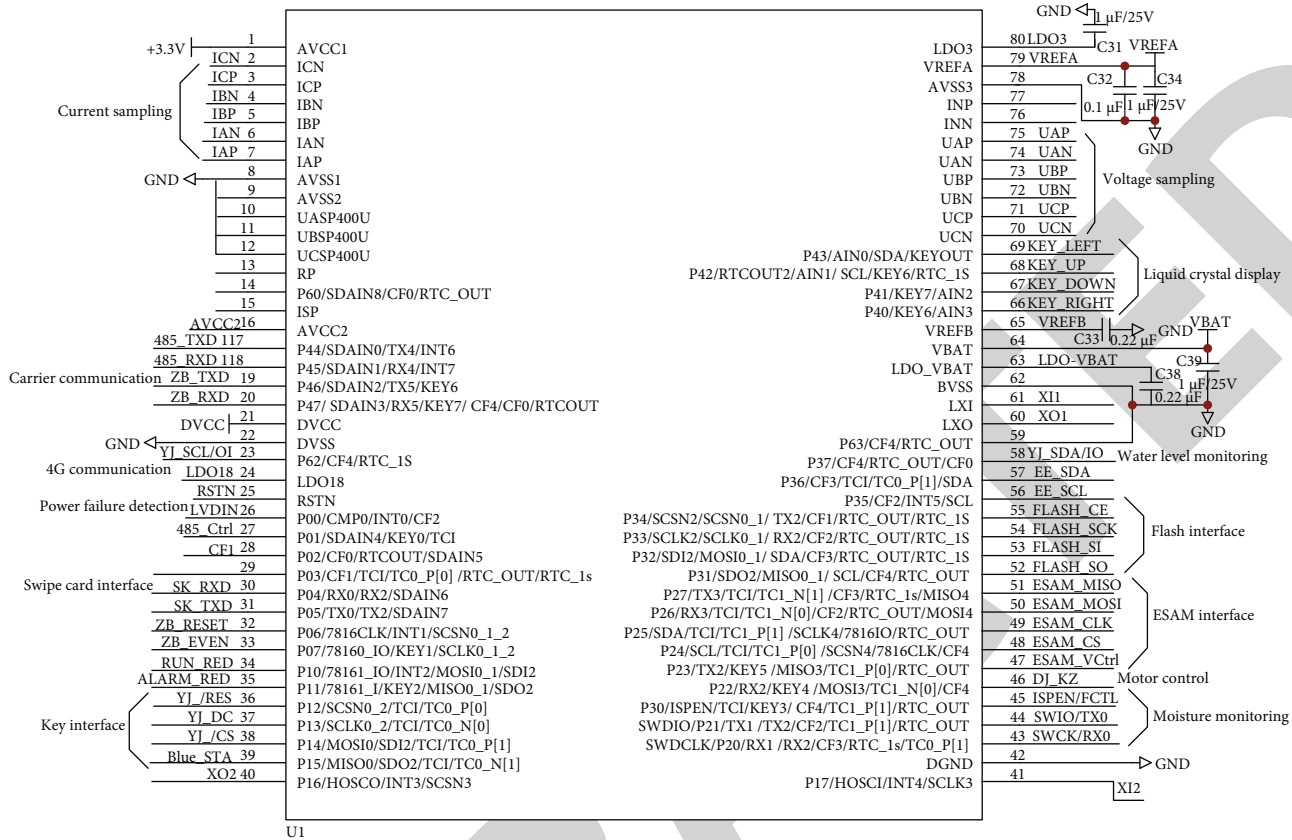


FIGURE 2: The main control circuit of intelligent measurement terminal.

module, EROM data storage, ESAM data encryption, 4G communication, HPLC broadband carrier communication, and other modules. See Figure 2 for details [12]. Under normal operation, the power consumption of the intelligent measurement terminal is about 0.05 W. In the slack season of irrigation, the intelligent measurement terminal automatically enters the sleep mode. The power consumption in the sleep mode is about 0.01 W, and all the power consumption costs are borne by the power company.

**3.2. The Power Supply Design Analysis.** The intelligent measurement terminal is generally installed at the end of the line in the low-voltage platform area, and voltage instability often occurs, so the reliability of the power module is required to be high. The power module adopts the switching power supply scheme design, using R231H switching power module, three-phase four-line width range AC power 275 V-475 V input, the output is 12 V DC voltage, the error is less than  $\pm 2\%$ , the output rated current is 280 mA, and the maximum output current is 350 mA. The power module supplies power to the HPLC broadband carrier module and outputs DC5V and DC3.3v voltages through JW5018 and SGM2203 DC step-down chips, respectively, to supply power to 4G module, RN2026, and other peripheral circuits. See Figure 3 for the detailed design principle [13].

In order to improve the reliability of the power module and prevent the impact of lightning short-term overvoltage on the intelligent measurement terminal, add varistors

VR1, VR2, and VR3 at the input end of the power module, and pass the surge test at the same time. In addition, in order to avoid damage to the power module caused by overvoltage during ground fault, MZ11-06E800 thermistor is added at the input end to ensure that the power module can recover automatically after the ground fault is removed.

**3.3. The Design of Data Storage Circuit.** The data storage of intelligent measurement terminal is composed of FLASH storage and EEPROM. FLASH storage is used to store fixed data such as device address, water price, electricity price, and user information [14]. FLASH memory adopts MAX25L6406 chip, the fast programming time is 0.6 milliseconds, the erasability and programming times are 100000, the data retention time is 20 years, and the data storage capacity is 64 KB, such as so FLASH\_CE, FLASH\_SO Interfaces are connected with RN2026 master chip. See Figure 4 for detailed circuit.

The design of EEPROM storage adopts CAT24C512WI chip, with a storage capacity of 512k, which is used to store dynamic data of intelligent measurement terminal, such as electric quantity data, power consumption record, fault record, and other data. See Figure 5 for the detailed design circuit.

**3.4. The Alternating Current Sampling Circuit.** Alternating current sampling circuit is the core circuit of intelligent measurement terminal, which is divided into voltage sampling

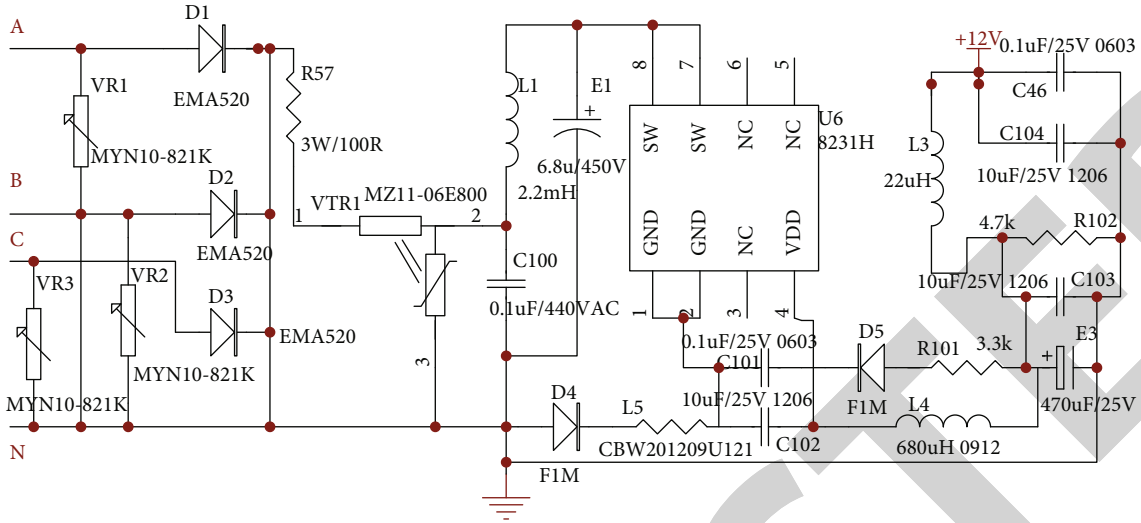


FIGURE 3: The power module circuit diagram.

and current sampling. The voltage sampling is composed of six 294 K and two 1 K high-precision voltage dividing resistors [15]. The voltage signals at both ends of the RA7 resistor are collected through the UAP and UAN pins of the microcontroller RN2026, and the phase A voltage is generated through analog-to-digital conversion.

Since the load of the intelligent measurement terminal is a high-power motor well pump, the high-precision 500:1 current transformer is used for current sampling. The input end of the transformer is connected with the transient diode Z1 and connected with the IAP and IAN of the microcontroller RN2026 through R1 and R3 step-down resistors and symmetrical RC filter circuit. The accuracy of voltage and current sampling is 0.2%. See Figure 6 for the detailed circuit [15]. This circuit module takes the voltage and current sampling of phase A as an example, and the principle of phase B and phase C is consistent with that of phase A.

**3.5. The Analysis of Card Swiping Circuit.** In the process of swiping cards to use electricity or water, users swipe cards frequently. If contact cards are used, repeated swiping of cards is likely to cause poor contact [16]. In order to improve the service life of cards and card readers, this card swiping circuit is designed with noncontact RF card reading technology. The induction coil is arranged inside the card [17]. Through the electromagnetic induction principle of the coil, the card balance, user information, etc. are read into the RN2026 microcontroller. The user can swipe the card normally only by putting the card close to the card reader. See Figure 7 for the detailed data interaction process [18].

## 4. The Function Design of Intelligent Measurement Terminal

**4.1. The Calculation Method of Irrigation Water Volume and Algorithm of “Water Conversion by Electricity” Coefficient.** The total water consumption in Hebei is mainly composed of groundwater, surface ditch water, natural precipitation, and water purchased from other regions [19]. After remov-

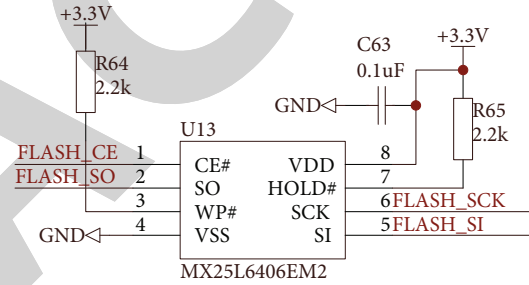


FIGURE 4: The FLASH storage circuit diagram.

ing daily domestic water, industrial production water, environmental protection water, and standby water, the remaining distributable water is agricultural irrigation water [20]. This study collected the amount of water resources, agricultural irrigation water consumption, and unit arable land water consumption in each city by collecting the official websites of municipal governments in Hebei region [21]. According to the principle of dynamic balance of water resources, taking the total amount of available water resources in the city area as the upper limit of water consumption in the city area, and based on the total amount of water used in various industries, the profit and loss balance relationship is calculated [22]. For urban areas where the total annual water consumption exceeds the local available water resources, the insufficient part shall be included in the adjustment of agricultural irrigation water, which shall be averaged to the total area of arable land in the whole urban area to obtain the adjustment amount of irrigation water per unit of arable land area [23]. Subtract the adjustment amount from the irrigation water consumption per unit of arable land area in the previous year to obtain the revised average water consumption authority per unit of arable land area in the current year. See the following formula for the detailed calculation method:

$$W_t = W_g + W_x + W_d + W_j. \quad (1)$$



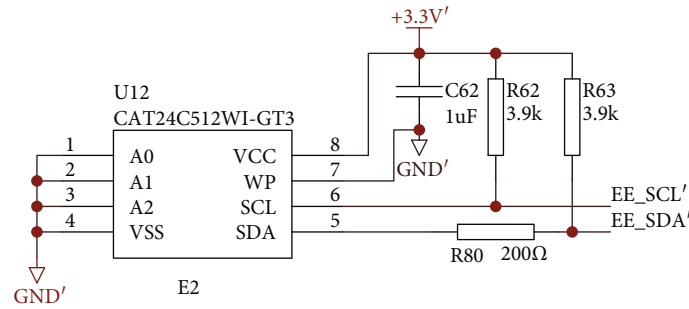


FIGURE 5: The EEPROM storage circuit diagram.

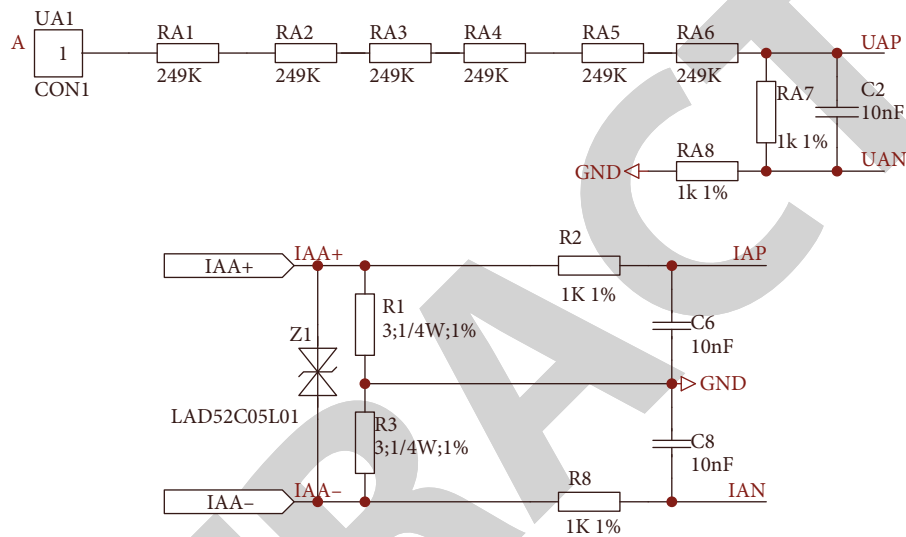


FIGURE 6: The alternating current sampling circuit diagram.

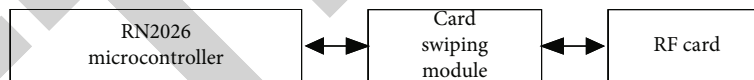


FIGURE 7: The card swiping data interaction diagram.

In formula (1),  $W_t$  is the total amount of water resources in an urban area,  $W_g$  is the water volume of surface ditches,  $W_x$  is the underground water volume,  $W_d$  is the purchased water volume, and  $W_j$  is the natural rainfall of the year; the unit of the above variables is  $m^3$ .

$$W_n = W_t - W_s - W_h - W_i - W_b. \quad (2)$$

In formula (2),  $W_n$  is the water consumption for agricultural production in an urban area,  $W_s$  is the domestic water consumption in an urban area,  $W_h$  is the water consumption for environmental protection,  $W_i$  is the industrial water consumption, and  $W_b$  is the reserve water consumption; the unit of the above variables is  $m^3$ .

$$\omega = \frac{W_n}{S_t}. \quad (3)$$

In formula (3),  $\omega$  is the irrigation water consumption per unit cultivated area, the unit is  $m^3 \cdot m^{-2}$ , and  $S_t$  is the total area of arable land in an urban area, the unit is  $m^2$ .

In order to solve the problem of lack of water metering facilities for motor well irrigation, the method of electricity to water coefficient is referred to as “water conversion by electricity,” and the water consumption of users can be calculated by measuring electricity alone [24]. According to the “water conversion by electricity” coefficient, the agricultural irrigation water consumption is calculated, and the optimized water consumption per unit of arable land is used as the upper limit of irrigation water. In the urban areas of Hebei Province, where groundwater or ditch water is used as irrigation water, the upper limit of irrigation water is the irrigation water consumption per unit of arable land. According to the “water conversion by electricity” coefficient calculated by the intelligent measurement terminal, and further based on the actual measured irrigation power consumption and the corresponding measured water volume

in Pingxiang County, Xingtai City, the above “water conversion by electricity” coefficient is verified. According to the geographical location of farmers’ cultivated land in Pingxiang County, the geographical location of motor wells used for irrigation, and the upper limit of water consumption per unit of arable land area corresponding to this location, the water consumption of each irrigation farmer is obtained by using the calculation coefficient of “water conversion by electricity,” and the intelligent measurement terminal is used to adjust the irrigation power consumption of each farmer as the control method of the total amount of irrigation water [25].

Through the intelligent measurement terminal, the data of pumping speed, pumping time, pump diameter, and so on of the pump in the motor well are collected, and the “water conversion by electricity” coefficient based on the water flow speed is calculated in a certain time. This coefficient is reused to other adjacent wells, and the water consumption is obtained by multiplying the power consumption each time by the “water conversion by electricity” coefficient, thus greatly reducing the investment cost of water metering facilities.

The calculation of the “water conversion by electricity” coefficient is divided into the following four steps. The first step is to calculate the cross-sectional area of the pumping pipeline. See formula (4) for the detailed calculation method.

$$S = \pi \times r^2. \quad (4)$$

In formula (4),  $S$  is the sectional area of the pumping pipeline, the unit is  $\text{m}^2$ ,  $\pi$  is the circumference, and  $r$  is the pipeline radius, the unit is  $\text{m}$ , which is determined according to the parameters indicated on the factory nameplate of the pump.

The second step is to calculate the pipe length. See formula (5) for the detailed calculation method.

$$L = v \times h. \quad (5)$$

In formula (5),  $L$  is the length of the pumping pipeline, the unit is  $\text{m}$ ,  $v$  is the water flow velocity, the unit is  $\text{m} \cdot \text{s}^{-1}$ , and  $h$  is the irrigation time, the unit is  $\text{H}$ .

The third step is to calculate the volume of irrigation water. See formula (6) for the detailed calculation method.

$$V = S \times L. \quad (6)$$

In formula (6),  $V$  is the volume of irrigation water, the unit is  $\text{m}^3$ ,  $S$  is the cross-sectional area of the pipe in formula (1), and  $L$  is the length of the pipe in formula (5).

The fourth step is to calculate the coefficient of “water conversion by electricity.” See formula (7) for the detailed calculation method.

$$\delta = \frac{V}{Q}. \quad (7)$$

In formula (7),  $\delta$  is the coefficient of “water conversion by electricity,”  $Q$  is the electricity generated within the irriga-

tion time  $h$ , the unit is  $\text{kWh}$ , and  $V$  is the volume of water used in formula (6).

By establishing the mode of standard wells, the “water conversion by electricity” coefficient of standard wells is distributed to other ordinary power consumption management terminals, and water metering and charging businesses can be carried out. If a water meter is installed at each measuring point to measure irrigation water consumption, the cost of water meter installation and maintenance is about CNY 5000 per year. Therefore, compared with the method of installing water meters, the cost of each measuring point can be saved about CNY 5000 by using the method of “water conversion by electricity.”

For the ditch irrigation mode, this method is also applicable, but the depth of the ditch should be considered when selecting the water pump, and the pump matching the depth of the ditch should be selected as far as possible to better ensure the accuracy of the “water conversion by electricity” coefficient.

*4.2. The Control and Management of Water and Electricity Charges.* The water charge is calculated by multiplying the water consumption by the water price with the method of “water conversion by electricity.” The water price is formulated and issued by Hebei Provincial Development and Reform Commission. The annual three-level quota water volume is allocated according to each  $666.67 \text{ m}^2$  of land. The first-level water price is  $P_1$ , the second-level water price is  $P_2$ , and the third-level water price is  $P_3$ ; the unit is  $\text{CNY} \cdot \text{m}^{-3}$ . For the applied water volume is  $S_1$ ,  $S_2$ , and  $S_3$ ; the unit is  $\text{m}^3$ ; the water price is set according to the principle of  $P_1 < P_2 < P_3$ . The water and electricity charges are controlled by the intelligent measurement terminal. The water and electricity prices are set in the terminal storage unit, or when the price changes, the water and electricity prices are distributed remotely through the electricity information acquisition system [26].

After the user starts to swipe the card to use electricity, the terminal will automatically settle the electricity consumption each time according to the start time, initial electricity consumption, end time, and end electricity consumption of each user [27]. According to the “water conversion by electricity” coefficient, the current water consumption is converted, and the current electricity and water consumption expenses are obtained according to the electricity price and water price set in advance. After the power consumption is completed, the terminal automatically deducts the water and electricity fees in the user’s electricity purchase card and returns the deducted balance to the user’s electricity purchase card [28]. See Figure 8 for the detailed process.

*4.3. The Control and Management of Water and Electricity Charges.* In this paper, the APSIM (agricultural production systems simulator) algorithm model is used to determine the soil moisture control index [28]. The algorithm model combines the management system, environmental conditions, crop growth characteristics, and other parameters and checks the actual parameters obtained based on the

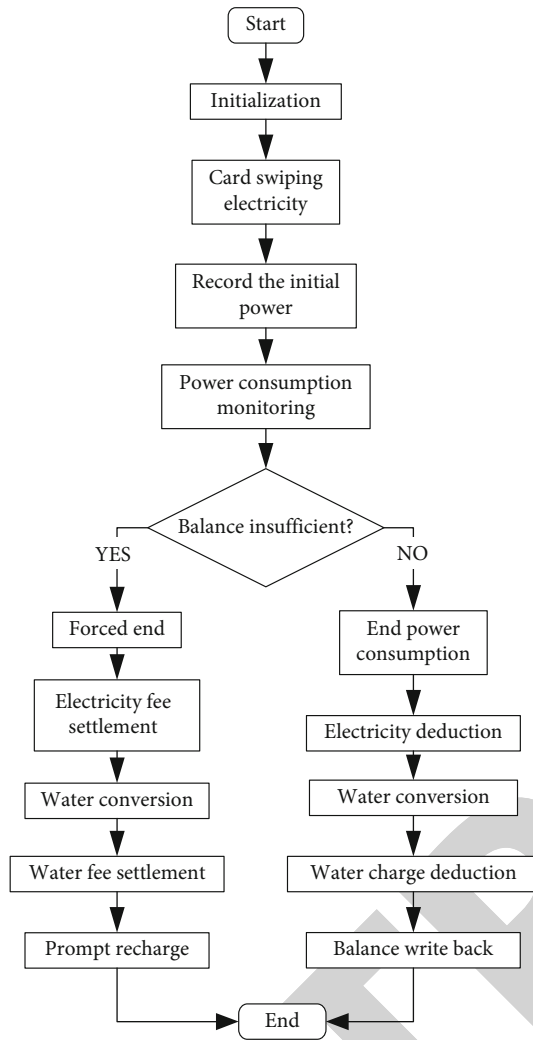


FIGURE 8: The control flow chart of water and electricity charges.

product of the above three parameters. The verified algorithm model can accurately predict the growth and yield of crops in the same environment. Based on the measured data of irrigation water for wheat, corn, and soybeans planted in Pingxiang County, Xingtai City, the APSIM algorithm model is validated, and the optimized algorithm model is used to calculate the growth and impact on yield under different irrigation water indicators. According to the simulation effect, the irrigation time, frequency, and water consumption of different crops are formulated to obtain the highest crop yield under the condition of optimal indicators.

The irrigation data for checking the APSIM model algorithm is from Pingxiang County, Xingtai City, and the validation time is from 2020 to 2021, a total of two crop growth seasons. The soil layer above 85 cm of the verification point is sandy soil, and the soil layer below 85 cm is clay. The average water content of soil above 1.8 m is about 34.6%, the wilting humidity is 9.8%, and the soil pH value is 7.8. During the observation period, the organic fertilizer content in the soil layer above 25 cm is 19~22 g.kg<sup>-1</sup>, the nitrogen content is 72~89 mg.kg<sup>-1</sup>, the phosphorus content is 22~39 mg.kg<sup>-1</sup>, and the potassium content is 87~118 mg.kg<sup>-1</sup>. When sowing

wheat in autumn, nitrogen (360~410 kg.hm<sup>-2</sup>), phosphorus (160~190 kg.hm<sup>-2</sup>), potassium (21 kg.hm<sup>-2</sup>), and other fertilizers are evenly spread on the surface of the farmland. Nitrogen fertilizer is applied to wheat, corn, soybeans, and other crops at the flowering and pollination period according to 25% of the sowing time. After soil tillage, the wheat weight is 148~190 kg hm<sup>-2</sup> sowing; using water sowing method, the spacing between rows is about 16 cm; corn is sown at equal intervals of 55 cm, with a density of 5.2~6.1 m<sup>-2</sup>.

The irrigation experiment using APSIM model needs to focus on three irrigation modes. The flowering and growth period of crops needs full irrigation (FI). Combined with the precipitation of the year, it generally needs to be irrigated 3-6 times. When the soil moisture is sufficient, the critical growth period of crops (CI, irrigation in critical period) can be irrigated once, under the condition of sufficient soil moisture and the minimum irrigation mode (MI) without irrigation in the key growth period. The irrigation water volume is set at 65~85 mm, which is normally treated as three times. The experimental field is randomly selected, and each area is about 4 m × 10 m. Different test fields are separated by more than 3 meters, and the construction of different test fields interferes with each other. The irrigation water is groundwater or ditch water, which is transported by circular pipes. The intelligent measurement terminal calculates the water consumption for each irrigation. During the experiment, the water consumption, power consumption, crop growth, and final output are recorded in detail.

The determination of the development period of wheat, corn, soybeans, and other crops is recorded according to the probability of 55% of the typical characteristics. Records of wheat growth density and dynamic changes are determined at 1 m in each test field 5 lines of regional records; record the harvest quantity of corn at harvest time, and calculate the harvest density. Install a 2.2 m deep neutron tube in each test field to regularly measure the water content of the 2.2 m soil layer. In the harvest period of crops, 90 stems of wheat, 3 soybeans, and 4 corn were selected for seed analysis in each experimental field; harvest all wheat, summer corn, and soybean plants in each test field mechanically, and measure the yield after each seed is naturally dried.

**4.4. Dynamic Balance Monitoring of Soil Water Content.** The dynamic balance monitoring method of soil water content is based on the dynamic balance of soil water content in the root layer of crops, combined with the weather and the actual growth of crops, to monitor the balance of soil water content, so as to determine the soil water content in the root layer of crops in different development periods and then compare it with the predetermined soil irrigation water index, judge whether the soil needs irrigation operation, and measure the amount of irrigation. Assuming that the runoff in the horizontal direction of the soil is ignored, the change of water content in the soil layer of crop root activity in a certain period of time is expressed by the following water content balance formula:

$$W_t = W_{t-1} + Y + G + X - H - L. \quad (8)$$



In formula (8),  $W_t$  is the farmland water content in the current period,  $W_{t-1}$  is the farmland water content in the previous period,  $Y$  is the natural rainfall in the current period,  $G$  is the irrigation water consumption in the current period,  $X$  is the water content of water vapor retained in the roots of crops in the current period,  $H$  is the crop growth consumption in the current period, and  $L$  is the soil leakage in the current period; the unit of the above variables is  $m^3$ . During dry weather, the amount of soil leakage can be ignored. Wheat, soybeans, corn, and other crops have great differences in root states in different growth cycles. It is predicted according to the length of crop growth.

$H$  is calculated according to the double coefficient method of crops. See formula (9) for details.

$$H = (K_b + K_z) \times H_0. \quad (9)$$

In formula (9),  $K_b$  is the crop foundation coefficient, which is affected by the crop leaf density and soil water content;  $K_z$  is the evapotranspiration coefficient, which is affected by the shallow soil water content;  $H_0$  is the standard evapotranspiration of crops, which is mainly affected by climatic conditions. The above three parameters are calculated according to the method of FAO-56 [29]. Soil moisture, climate change, crop evapotranspiration, and other data are monitored and collected in real time by the intelligent measurement terminal. According to the preset irrigation strategy, irrigation decision-making events are generated and reported to the electricity information system through the 4G communication module. The system sends them to farmers to guide farmers in precision irrigation. Farmers can view the irrigation strategy pushed by the system through the mobile phone APP and carry out farmland irrigation or fertilization by referring to the irrigation strategy. Farmers can feed back the rationality of irrigation strategies through mobile APP, and the system continuously optimizes the irrigation strategies according to the feedback of farmers to form a good interaction mechanism.

## 5. Experimental Verification

**5.1. The Error Verification of “Water Conversion by Electricity” Coefficient.** The coefficient of “water conversion by electricity” is the linear relationship between farmers’ irrigation power consumption and water consumption. The water consumption is calculated according to the power consumption and used to collect water charges. As long as the given water consumption per  $666.67 m^2$  of farmland is converted into the given power consumption, the total water consumption can be adjusted. The coefficient of “water conversion by electricity” is the core parameter of regulating groundwater extraction by using intelligent measurement terminal. According to the irrigation power and water consumption data of farmers’ motor wells in Pingxiang County, Xingtai City, the accuracy of the “water conversion by electricity” coefficient under different regional motor wells and irrigation modes is analyzed. The results show that in a small range, the shallow groundwater level, hydrogeological environment, and motor well conditions are not different, the

“water conversion by electricity” coefficient of different farmers’ motor wells is relatively stable, and the pump lift, the power, and the difference of parameters such as water flow velocity and irrigation mode are the main influencing conditions. This paper selects 10 agricultural machine wells in Pingxiang County, Xingtai City, to verify the “water conversion by electricity” coefficient at different groundwater levels. When the water level of 10 agricultural machine wells is 45 meters, the “water conversion by electricity” coefficient is between  $3.55 m^3 \cdot kWh^{-1}$  and  $3.63 m^3 \cdot kWh^{-1}$ ; the coefficient is between  $4.95 m^3 \cdot kWh^{-1}$  and  $5.33 m^3 \cdot kWh^{-1}$  when the groundwater level is 30 meters and between  $9.90 m^3 \cdot kWh^{-1}$  and  $9.98 m^3 \cdot kWh^{-1}$  when the groundwater level is 15 meters. The above results show that the “water conversion by electricity” coefficient is relatively stable, which is consistent with the rated working parameters of the pump of the motor well, but different irrigation modes such as sprinkler irrigation, canal irrigation, and pipe irrigation have the greatest impact on this coefficient. The detailed results are shown in Figure 9. The horizontal axis in the figure represents the irrigation power consumption of farmers, and the vertical axis represents the water consumption. Three different types of water pumps are used to select the power consumption records of 10 households. The results obtained through linear fitting show that the water consumption is obtained by multiplying the electricity quantity by the coefficient of “water conversion by electricity.” In practical application, it needs to be adjusted according to the irrigation mode.

**5.2. The Estimation Results of Average Water Use Authority per Unit Arable Area.** Allocating the total water consumption in a city area to the unit arable land area and determining the upper limit of irrigation water per unit arable land are important measures to optimize the agricultural irrigation water resource management system and improve the efficiency of water resource management [30]. By collecting the recent total water resources and agricultural irrigation water consumption of the county from the official website of the county, it is estimated that the available amount of shallow groundwater in Hebei is  $664 \sim 2984 m^3 \cdot hm^{-2}$ . According to the existing total water consumption of various industries and the accounting balance relationship, for counties and cities where the actual total water consumption exceeds the standard available water, the part exceeding the standard will be supplemented by agricultural irrigation water, the total amount of agricultural irrigation available water in the county after reduction will be calculated, and then, it will be evenly distributed to the arable land unit area, and based on this, the average water authority per unit arable land area after reduction will be obtained. See Table 1 for details.

According to the data in Table 1, Shijiazhuang has the largest average available water per unit of arable land, followed by Baoding and Handan, and Cangzhou has the least. In the same prefecture level city, the largest difference in the water volume per unit of arable land area in different counties and districts is Cangzhou area, from the smallest  $664 m^3 \cdot hm^{-2}$  to the largest  $1918 m^3 \cdot hm^{-2}$ . The water volume per unit of arable land area in different areas varies greatly.

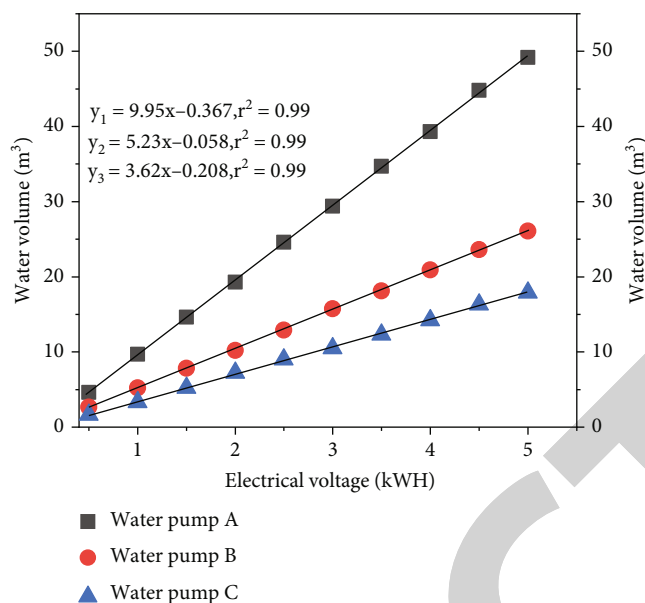


FIGURE 9: The verification results of “water conversion by electricity” coefficient.

TABLE 1: The cultivated land area irrigated by groundwater and water consumption per unit arable area in Hebei region.

City	Cultivated land area ( $\times 10^4$ hm <sup>2</sup> )	Water consumption per unit area (m <sup>3</sup> ·hm <sup>-2</sup> )		
		Average value	Maximum	Minimum
Xingtai	58.26	1751.0	2882	1230
Baoding	57.35	2077.6	2984	1368
Handan	60.61	2041.4	2695	1258
Cangzhou	70.38	1191.3	1918	664
Hengshui	57.35	1783.7	2307	1018
Shijiazhuang	43.86	2589.5	2954	2041

The annual water consumption of wheat, corn, soybeans, and other crops in Hebei is between 740 and 860 mm [30], and the available irrigation water consumption can provide about 9%-38% of the crop water consumption. The available water volume in different urban areas and counties is inconsistent, and the water authority per unit arable land area and the appropriate irrigation mode need to be determined according to the actual situation [31].

**5.3. The Verification of Dynamic Equilibrium Prediction Method of Soil Water Content.** The dynamic balance method of soil water content in formula (8) is compared with the actual measured dynamic change of soil water content to evaluate the reliability of predicting the result of soil water content by using the dynamic balance method of soil water content [32]. The daily evapotranspiration (ET<sub>0</sub>) of wheat, corn, and soybeans during the growth period from 2019 to 2020 and the actual evapotranspiration under different irrigation modes are shown in Figure 10. The leaf index of wheat, corn, and soybean in the growth period of minimum irrigation period, critical period, and full irrigation period was significantly different in the middle and late development period; affected by the size of crop canopy and the change of soil moisture, the daily evapotranspiration of the

three irrigation cycles gradually increased in different growth periods. The total water consumption of wheat in the minimum irrigation period, critical irrigation period, and full irrigation period is 284.3 mm, 388.1 mm, and 533.2 mm, respectively, and that of corn is 212.4 mm, 278.2 mm, and 388.5 mm, respectively. The water content conditions of the three irrigation periods are obviously different, which provides a basic condition for verifying the reliability of the prediction method of soil water dynamic balance [33].

Using the dynamic balance formula (8) of soil water content and the double crop estimation coefficient method of actual crop water consumption provided by FAO56 [34], the average root water content of wheat, corn, and soybeans under three irrigation modes from 2019 to 2020 is calculated. Among them, the root depth of wheat, corn, and soybean in different growth cycles is between 0 and 1.5 m. The maximum evaporation depth of soil water is calculated as 15 cm, and the lower limit of crop water consumption without water deficit is calculated as 56% of the total effective soil water content for wheat, 51% for corn, and 48% for soybeans.

According to the long-term observation data of Pingxiang County, Xingtai City, the crop coefficients of wheat, corn, and soybean in different growth cycles are between 0.59 and 0.95 when there is no water deficit. When the soil

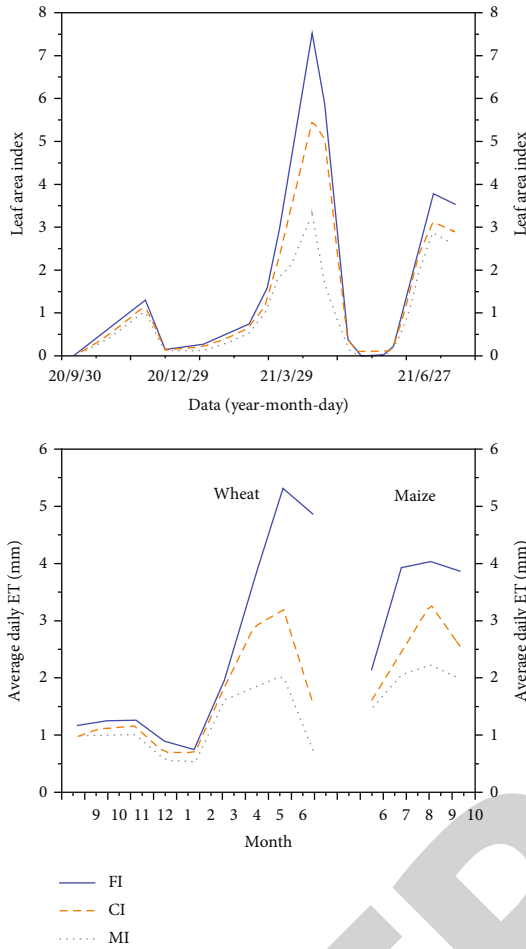


FIGURE 10: The change of actual evapotranspiration under different irrigation modes.

water content of crop roots is lower than 43% (wheat) and 48% (corn) of the effective value, the crop root coefficient will show a linear decreasing trend according to the decline of water content [35]. When the root soil moisture content decreases to the wilting moisture content, the crop coefficient is 0. The average water holding capacity of 2 m soil layer in Pingxiang County is calculated as 34%, and the wilting water content is 11%. The results of the model algorithm simulation and the daily average soil water content using the intelligent measurement terminal under different irrigation modes are shown in Figure 11. The correlation coefficient between the simulated value and the measured daily soil water content under the three irrigation modes is between 0.94 and 0.96, and the similarity between the two is high, indicating that the above method can accurately predict the change of root soil water content to guide farmers' irrigation decisions.

**5.4. The Performance Verification of Intelligent Measurement Terminal.** In order to verify the accuracy of the measurement error of the motor well irrigation measurement terminal, the experiment is carried out according to the requirements of GB/T 17626.3-2016 radio frequency electro-

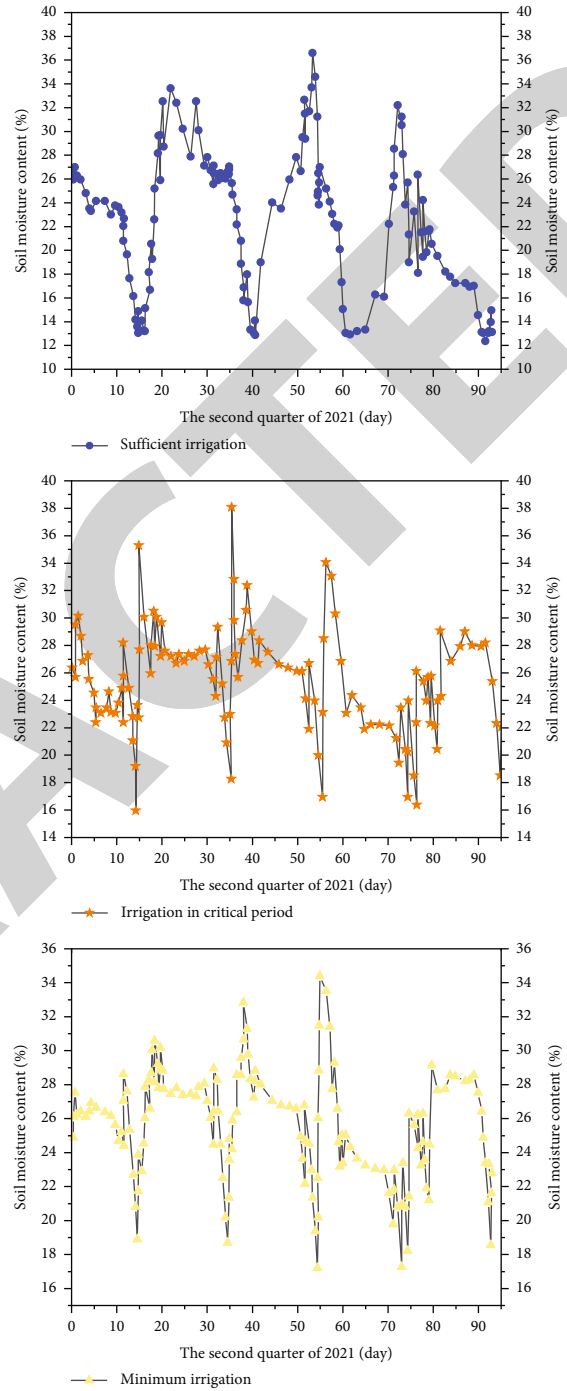


FIGURE 11: The daily average soil water content change.

magnetic field radiation immunity standard. The experimental ambient temperature is 23°C, the experimental field strength is 10 V/m and 30 V/m, and the sample direction is the front, side, and top surface. 80 MHz-2000 MHz pulse signal is applied during the experiment.

During the experiment, five measurement error data were recorded at each frequency point. After the above experiment, the terminal error of pumping well irrigation measurement was less than 0.5%, which increased by 1.15% compared with the measurement error of 1.65% in

TABLE 2: The electric energy measurement error data record form.

Frequency	Error data (%)				
80 MHz	0.32	0.25	0.45	0.42	0.40
200 MHz	0.37	0.35	0.42	0.37	0.47
500 MHz	0.27	0.25	0.45	0.42	0.40
1000 MHz	0.37	0.32	0.50	0.47	0.45
2.0 GHz	0.42	0.40	0.47	0.47	0.49

literature [36], meeting the expected goal. See Table 2 for the detailed records of some error data.

## 6. Conclusion

In this paper, an intelligent measurement terminal device based on RN2026 microcontroller is designed. The function and performance of the intelligent measurement terminal are verified by experiments. The results show that (1) the coefficient of “water conversion by electricity” based on water flow speed is more stable, and the coefficient error is less than 1%, which is basically consistent with the rated working parameters of different types of well water pumps. (2) The estimation result of average water use right per unit of arable land area is basically consistent with the actual situation of various cities in Hebei. Shijiazhuang City has the largest average available water volume of arable land area, while Cangzhou City has the smallest. (3) The predicted results of soil moisture dynamic balance are consistent with the daily average soil moisture change and the actual evapotranspiration change trend under different irrigation modes, and the correlation coefficient between the simulated value and the measured daily soil moisture is 0.94~0.96. (4) The measurement error of the intelligent measurement terminal is less than 0.5%, meeting the test requirements of GB/T 17626.3-2016 RF electromagnetic field radiation immunity standard. (5) Compared with the traditional irrigation mode, the intelligent measuring terminal can save 12 m<sup>3</sup> of water per 0.067 hm<sup>2</sup>.

The intelligent measuring terminal of water-saving irrigation is mainly used in the pump well irrigation mode. This paper mainly studies the method of “water conversion by electricity” coefficient based on water flow speed, the establishment of water right constraint mechanism, the determination of soil moisture control index, and the monitoring method of soil moisture dynamic change. Compared with other water-saving irrigation equipment, the biggest advantage is to automatically generate irrigation strategies based on the groundwater level, soil moisture, and crop growth status to guide farmers to conduct scientific irrigation and achieve good application results.

The current research on intelligent measurement terminals mainly focuses on the electricity use scenarios of agricultural irrigation card swiping, while in practical applications, there are electricity use scenarios of public rental houses, commercial streets, and other public places. In the future, we will study the intelligent power technology under different application scenarios, improve the intelligent level

of equipment through remote code scanning, and meet the application requirements of different scenarios.

## Data Availability

All data, models, and code generated or used during the study appear in the submitted article.

## Conflicts of Interest

The authors declare that they have no conflicts of interest.

## Acknowledgments

This work is supported by the State Grid Hebei Electric Power Company Science and Technology Project (ks2021-034-II).

## References

- [1] H. P. Luo and X. L. Huang, “Water resource use and effects in grain production in the major crop grown regions in China,” *Agricultural Economy*, vol. 2, pp. 3–5, 2020.
- [2] W. A. N. G. Hongxi, L. I. Hongjun, and Q. I. Yongqing, “Development of a decision support system for irrigation management to control groundwater withdrawal,” *Chinese Journal of Eco-Agriculture*, vol. 30, no. 1, pp. 138–152, 2022.
- [3] W. A. N. G. Mingfei, T. I. A. N. Hongwu, Z. H. A. N. G. Shirui, and L. I. Jinlei, “Design and development of remote water and electricity metering equipment for farm pumped wells,” *Jiangsu Agricultural Sciences*, vol. 45, no. 13, pp. 177–180, 2017.
- [4] L. I. Wen, K. Huang, Z. H. A. N. G. Qingfang, G. U. O. Kai, and X. U. Minggang, “Intelligent double control system of water and electricity for agricultural irrigation well house,” *Journal of Henan University of Science and Technology*, vol. 40, no. 3, pp. 73–79, 2019.
- [5] L. I. U. Hongyan, Z. Mingwei, and W. Chun, “Intelligent control system design of wireless irrigation for seedling based on ARM and STM32,” *Journal of Agricultural Mechanization Research*, vol. 39, no. 1, pp. 132–136, 2017.
- [6] G. H. Zhang, Y. L. Lian, C. H. Liu, M. J. Yan, and J. Z. Wang, “Situation and origin of water resources in short supply in North China Plain,” *Journal of Earth Sciences and Environment*, vol. 33, no. 2, pp. 172–176, 2011.
- [7] D. L. Wang and G. H. Zhang, “Groundwater ensure capacity spatial-temporal characteristics and mechanism in main grain producing areas of North China Plain under different climatic conditions,” *Acta Geoscientica Sinica*, vol. 38, no. S1, pp. 47–50, 2017.
- [8] K. Tan, S. Fang, G. Zhou, S. Ren, and J. Guo, “Responses of irrigated winter wheat yield in North China to increased temperature and elevated CO<sub>2</sub> concentration,” *Journal of Meteorological Research*, vol. 29, no. 4, pp. 691–702, 2015.
- [9] F. A. N. Hongmei, L. I. U. Xiaomin, W. A. N. G. Wenjuan, and C. H. E. N. Qiong, “Estimating water consumption from electricity consumption: how to calculate the conversion coefficient,” *Journal of Irrigation and Drainage*, vol. 40, no. 11, pp. 98–105, 2021.
- [10] F. Chen, Y. Y. Ding, Y. Y. Li et al., “Practice and consideration of groundwater overexploitation in North China Plain,”



- South-to-North Water Transfers and Water Science & Technology*, vol. 18, no. 2, pp. 191–198, 2020.
- [11] H. Y. Sun, X. Y. Zhang, E. L. Wang, S. Chen, and L. Shao, “Quantifying the impact of irrigation on groundwater reserve and crop production - a case study in the North China Plain,” *European Journal of Agronomy*, vol. 70, no. 8, pp. 48–56, 2015.
- [12] L. I. U. Shao, “Water pricing towards sustainability of water resources: a case study in Beijing,” *Journal of Environmental Sciences.*, vol. 14, no. 4, pp. 518–523, 2002.
- [13] C. H. E. N. Cai-ming, L. I. Qi-feng, and C. H. E. N. Xin, “Research on the statistical method of irrigation water consumption for farmland based on “conversion of electricity to water” and irrigation return water,” *China Rural Water and Hydropower*, vol. 19, no. 9, pp. 68–71, 2019.
- [14] M. Wu, F. Lan, and L. Xie, “Methods in underground water withdraw amount decided by electricity use,” *Hebei Water Resources*, vol. 8, pp. 30–31, 2019.
- [15] J. Y. Wang, “Affordability in water price reform for underground water irrigation regions in Hebei,” *Haihe Water Resources*, vol. 23, no. 6, pp. 59–61, 2017.
- [16] X. Y. Zhang, “Water use and water-saving irrigation in typical farmlands in the North China Plain,” *Chinese Journal of Eco-Agriculture*, vol. 26, no. 10, pp. 1454–1464, 2018.
- [17] S. S. Liang, J. X. Guan, L. Li, and L. W. Shao, “Impact of irrigation schedules on yield, water consumption and water use efficiency of winter wheat,” *Journal of Irrigation and Drainage*, vol. 38, no. 5, pp. 52–59, 2019.
- [18] X. Xu, M. Zhang, J. Li et al., “Improving water use efficiency and grain yield of winter wheat by optimizing irrigations in the North China Plain,” *Field Crop Research*, vol. 221, no. 4, pp. 219–227, 2018.
- [19] Y. U. Meixiu, D. O. N. G. Wuxin, Z. H. A. N. G. Jianyun, W. E. I. Li, W. U. Zhi, and W. A. N. G. Guoqing, “Agricultural drought of the Poyang Lake basin based on large -scale ground monitoring of soil water content,” *Advances in Water Science*, vol. 33, no. 2, pp. 185–195, 2022.
- [20] L. Xiaoyin, G. Mingyi, Z. Xinyi, and X. Junzeng, “Enforcing energy balance closure by evaporation ratio method and its effect on evapotranspiration estimation of paddy fields,” *Transactions of the Chinese Society of Agricultural Engineering*, vol. 37, no. 11, pp. 121–130, 2021.
- [21] Y. Ning, Z. Qiang, and Z. Qiguo, “About single phase smart electricity meters remote switching function testing technology research,” *Electrical Measurement & Instrumentation*, vol. 53, no. 51, pp. 165–169, 2016.
- [22] W. Xiqin, Z. Xinyue, and C. Hao, “Irrigation water consumption and water - saving potential of food crops in groundwater over - exploitation areas in North China: based on survey data of 620 households in Hebei Province,” in *Journal of Northwest University*, vol. 50, no. 2pp. 227–233, Natural Science Edition, 2020.
- [23] P. Juntao, G. Xiaoxuan, and C. Jun, “Time synchronization of cost control electricity meter considering the information security interaction mode,” *Electrical Measurement & Instrumentation*, vol. 55, no. 22, pp. 147–152, 2018.
- [24] W. Kai and D. Zhenliang, “Design and implementation of charge control metering device in low voltage,” *Applications*, vol. 38, no. 6, pp. 162–164, 2021.
- [25] G. Bo, G. Yuan, and L. Fei, “Application analysis and optimization of object oriented smart watt-hour meter remote fee control,” vol. 39, no. 4, pp. 35–36+42, 2020.
- [26] L. I. Fen, X. I. E. Zhiwei, and Z. H. A. N. G. Qichang, “Design of the intelligent acquisition module of three-fee-controlled electricity meter based on 4G,” *Electronics*, vol. 49, no. 3, pp. 18–22, 2020.
- [27] S. Saadi, V. Simonneaux, G. Boulet et al., “Monitoring irrigation consumption using high resolution NDVI image time series: calibration and validation in the Kairouan Plain (Tunisia),” *Remote Sensing*, vol. 7, no. 10, pp. 13005–13028, 2015.
- [28] Y. Q. Huang, D. Wang, and X. N. Chen, “Design of soil moisture monitoring and irrigation forecast system,” *Water Saving Irrigation*, vol. 34, no. 5, pp. 13–15, 2008.
- [29] H. J. Li, J. Z. Li, Y. J. Shen, X. Zhang, and Y. Lei, “Web-based irrigation decision support system with limited inputs for farmers,” *Agricultural Water Management*, vol. 210, no. 7, pp. 279–285, 2018.
- [30] S. Y. Ma, M. Y. Sun, Y. H. Fu, Z. B. Jia, and S. Li, “Methods and practice use of water right confirmation in Hebei Province,” *South-to-North Water Transfers and Water Science & Technology*, vol. 17, no. 4, pp. 94–103, 2019.
- [31] Z. Z. Yan, X. Y. Zhang, M. A. Rashid, H. Li, H. Jing, and Z. Hochman, “Assessment of the sustainability of different cropping systems under three irrigation strategies in the North China Plain under climate change,” *Agricultural Systems*, vol. 178, no. 8, article 102745, 2020.
- [32] R. G. Allen, L. S. Pereira, D. Raes, and M. Smith, *Crop Evapotranspiration — Guidelines for Computing Crop Water Requirements — FAO Irrigation and Drainage Paper 56[EB/OL]*, FAO, Roma, 1998.
- [33] R. G. Allen, L. S. Pereira, M. Smith, D. Raes, and J. L. Wright, “FAO-56Dual crop coefficient method for estimating evaporation from soil and application extensions,” *Journal of Irrigation and Drainage Engineering*, vol. 131, no. 1, pp. 2–13, 2005.
- [34] X. L. Liang, W. Lyu, and F. Lan, “Factors affecting the electricity water conversion coefficient — the effects of irrigation methods,” *Haihe Hydrology*, vol. 26, no. 1, pp. 68–70, 2020.
- [35] H. J. Wang and X. Y. Zhang, “Evaluating the comprehensive effects of planting winter wheat in the groundwater depletion regions in the North China Plain,” *Chinese Journal of Eco-Agriculture*, vol. 28, no. 5, pp. 724–733, 2020.
- [36] L. Yuanlong, P. Jun, W. A. Wei, Z. Shengpeng, and X. Zongyi, “Research on intelligent sensing terminal technology of a distribution transformer for ubiquitous power internet of things,” *Power System Protection and Control*, vol. 48, no. 16, pp. 140–146, 2020.